Retreat of the Antarctic Ice Sheet during the Last Interglaciation and implications for future change

N. R. Golledge[1], P. U. Clark[2,3], F. He[4], A. Dutton[5], C. S. M. Turney[6,7,8], C. J. Fogwill[6,9], T. R. Naish[1], R. H. Levy[1,10], R. M. Mckay[1], D. P. Lowry[10], N. A. N. Bertler[1,10], G. B. Dunbar[1], A. E. Carlson[11]

[1]Antarctic Research Centre, Victoria University of Wellington, Wellington 6140, New Zealand
[2]College of Earth, Ocean, and Atmospheric Sciences, Oregon State University, Corvallis, OR, USA
[3]School of Geography and Environmental Sciences, University of Ulster, Coleraine, UK
[4]Center for Climatic Research, Nelson Institute for Environmental Studies, University of Wisconsin-Madison, Madison, WI, USA
[5]Department of Geoscience, University of Wisconsin-Madison, Madison, WI, USA
[6]Palaeontology, Geobiology and Earth Archives Research Centre, School of Biological, Earth and Environmental Sciences, University of New South Wales, Kensington NSW 2033, Australia
[7]Australian Research Council Centre of Excellence in Australian Biodiversity and Heritage, School of Biological, Earth and Environmental Sciences, University of New South Wales, Kensington NSW 2033, Australia
[8]Chronos 14 Carbon-Cycle Facility, University of New South Wales, Sydney NSW 2052, Australia
[9]School of Geography, Geology and the Environment, Keele University, Staffordshire ST5 5BG, United Kingdom
[10]GNS Science, Avalon, Lower Hutt 5011, New Zealand
[11]Oregon Glaciers Institute, Corvallis OR 97330, USA

Key Points:

- We present data-constrained simulations of the Antarctic Ice Sheet during the Last Interglaciation
- Our model predicts a maximum contribution to global mean sea level of 4 m at 126 ka BP
- Loss of much of the present-day West Antarctic Ice Sheet is already committed under current climate

Corresponding author: Nicholas R. Golledge, `nicholas.golledge@vuw.ac.nz`

Abstract

The Antarctic Ice Sheet (AIS) response to past warming consistent with the 1.5–2°C 'safe limit' of the United Nations Paris Agreement is currently not well known. Empirical evidence from the most recent comparable period, the Last Interglaciation, is sparse, and transient ice-sheet model simulations are few and inconsistent. Here we present new results from transiently-forced ice-sheet modelling experiments. We evaluate our results against near and far-field proxy reconstructions and find good agreement. Our simulations indicate that the AIS contributed approximately 4 m to global mean sea level, peaking at 126 ka BP, with ice lost primarily from the Amundsen but not Ross or Weddell Sea sectors. The AIS thinned in the area of the Wilkes Subglacial Basin but did not retreat. Continuing beyond present day our model predicts that the West Antarctic Ice Sheet may already be predisposed to collapse even in the absence of further environmental change.

Plain Language Summary

Ice sheets can respond to climatic warming in complex ways, commonly only reaching a new state of balance many hundreds or even thousands of years after the initial change in climate has occurred. Here we investigate how the Antarctic Ice Sheet responded to a period of prolonged warmer-than-present climate that took place around 125000 years ago. At this time the global climate was only around 1 to 2°C above present, but geological records show that global sea level was at least 6 m, or maybe even as much as 9-11 m, higher than today. Our study shows that around 4 m of this could have come from Antarctica. Our model agrees well with geological evidence of enhanced ice discharge both close to the ice sheet and further afield. Applying this model to the future our experiments suggest that the West Antarctic Ice Sheet may already have been sufficiently destabilised to trigger a long-term sea level contribution of up to 4 m, even without further greenhouse gas emissions.

1 Introduction

Direct evidence of ice sheet changes during the last time when global mean sea level (GMSL) was above present is sparse. This period, the Last Interglaciation (LIG, 129–116 ka BP) was most likely characterised by a highstand in GMSL of 6–9 m (Masson-Delmotte et al., 2013; Dutton et al., 2015) or higher (Rohling et al., 2019), but global

mean surface temperatures (GMST) only slightly elevated (ca. +0.8°C) with respect to early industrial times (late 19th century) (Turney & Jones, 2010; Masson-Delmotte et al., 2013; Fischer et al., 2018). GMST was amplified in the polar regions, with Arctic surface temperature anomalies of >3–11°C, substantially above the global mean (Landais et al., 2016; Yau et al., 2016; Fischer et al., 2018). Summer insolation was greater than at present (early 21st century) in the Northern Hemisphere during the early part of the LIG (peak ca. 127 ka), but reached a maximum in the Southern Hemisphere half a precession cycle later, at around 117 ka (Capron et al., 2017). Global mean ocean temperatures reached their maximum early in the LIG (129–127 ka BP) reaching 1.1±0.3°C above modern (approximately 2°C above early industrial; Shackleton et al., 2020), with extratropical southern hemisphere mean annual sea surface temperatures most likely peaking before those in the northern hemisphere (Hoffman et al., 2017). Southern Ocean summer sea surface temperature anomalies were around 1.8±0.8°C above pre-industrial (Capron et al., 2017). Around Antarctica, ocean temperatures reached their maxima at different times in different areas, with earliest warming (ca. 129–127 ka BP) in the Atlantic and Indian Ocean sectors, and delayed warming (ca. 125 ka BP) in the Pacific sector (Chadwick et al., 2020). Warming of subsurface layers relative to glacial maximum conditions exceeded surface warming during the LIG, and was most likely a consequence of a prolonged period of relatively weak Atlantic Meridional Overturning Circulation during the penultimate deglaciation (Marino et al., 2015; Clark et al., 2020; Turney et al., 2020).

Partitioning of ice sheet contributions to the inferred LIG highstand is hampered both by sparse evidence and by model disagreement. Thermal expansion of the ocean early in the LIG accounts for ca. 0.8 m sea-level-equivalent (SLE) change (Shackleton et al., 2020) and global glaciers could have contributed a maximum of 0.32 ± 0.08 m based on estimates of their current volume (Marzeion et al., 2020). The SLE contribution from the Greenland Ice Sheet (GrIS) is modelled to be anywhere from ca. 0.9 m (Clark et al., 2020) to ca. 5.1 m (Yau et al., 2016), with the majority of models and proxy-based reconstructions indicating likely mass loss in the 1–2 m SLE range (Colville et al., 2011; Dahl-Jensen et al., 2013; Calov et al., 2015; Goelzer et al., 2016; Bradley et al., 2018). The Antarctic Ice Sheet (AIS) has been less well studied, particularly in terms of ice sheet model (ISM) simulations that use ocean–atmosphere boundary conditions directly from general circulation models (GCM) or regional climate models (RCM). Whole-continent ISM reconstructions that have used environmental forcings directly from climate mod-

els without the imposition of additional heat predict an AIS LIG contribution of 3–4.4 m (Goelzer et al., 2016; Clark et al., 2020) whereas models that have used mid-latitude proxy-based sea surface temperatures, or temperature anomalies added to modelled values, predict similar or slightly higher SLE contributions of 3–7.5 m (Sutter et al., 2016; DeConto & Pollard, 2016). Whole continent as well as single catchment or limited area models have been used to investigate the sensitivity of key AIS drainage basins to both realistic and conceptual warming levels (Mengel & Levermann, 2014; Feldmann & Levermann, 2015; Golledge, Levy, et al., 2017; Sutter et al., 2020) but the scarcity of near-field empirical evidence with which to constrain ISM simulations prevents a critical evaluation of either the LIG AIS contribution to GMSL or the robustness of the models themselves.

To-date, direct indicators of AIS response during the LIG are limited to a horizontal ice core record from the Patriot Hills (West Antarctica) (Turney et al., 2020) and a marine sediment record from the continental shelf proximal to the Wilkes Subglacial Basin (WSB, East Antarctica) (Wilson et al., 2018). The Horseshoe Valley blue ice record (Turney et al., 2020) incorporates volcanic glass geochemically correlated with tephra in the Dome Fuji ice core, dated to 130.7 $\pm$ 1.8 ka BP (AICC2012 timescale; Hillenbrand et al., 2008), abruptly truncated by a hiatus in ice accumulation until ca. 80 ka BP. This hiatus is interpreted as evidence of dynamic thinning of this sector of the ice sheet during, and following, the LIG (Turney et al., 2020). By contrast, ice core records from the dynamically stable continental interior record only minor isotopic deviations reflecting temperature and/or elevation change (Korotkikh et al., 2011), and cores from sites more likely to have been substantially influenced by ice sheet retreat are typically too short to preserve an unambiguous LIG record (Brook et al., 2005; Fudge et al., 2013; Mulvaney et al., 2014; Buizert et al., 2015). The marine sediment core offshore the WSB at U1361A reveals a clear signal of increased iceberg rafted debris (IBRD) over the site during the LIG, which together with provenance indicators from muds eroded off the continental margin suggests either a retreat of the ice margin in the WSB, or an increase in basal erosion and sediment transport from this area (Wilson et al., 2018). Other, indirect, proxy records appear to show that the EAIS in this sector has been stable for at least the last 400 kyr (Blackburn et al., 2020), implying no retreat of ice in the WSB during the LIG.

No whole-continent AIS simulations have yet been explicitly assessed in terms of their agreement with ice-sheet proximal empirical interpretations. In this paper we there-

fore aim to 1) present new ISM simulations for the period 140–116 ka BP, and 2) compare modelled changes with those inferred from ice-proximal and ice-distal proxy reconstructions described above. Based on these results we are then able to make an assessment of the level of model–data agreement for the LIG, and on the basis of this, make inferences regarding future grounding-line retreat and AIS mass loss.

2 Methods

We use the same ice sheet model as used in Clark et al. (2020) but with modifications to improve model–data agreement. In summary, we use the Parallel Ice Sheet Model (PISM; Bueler & Brown, 2009; Winkelmann et al., 2010), a fixed-grid thermodynamic ice sheet model that uses a hybrid stress balance combining shallow approximations of the flow equations for grounded and floating ice. PISM is well-suited to multi-millennial simulations and has been used extensively for such purposes (Seguinot et al., 2014; Golledge et al., 2014; Winkelmann et al., 2015; Aschwanden et al., 2019; Albrecht et al., 2020). We implement the model at 20 km horizontal resolution and make use of the native subgrid grounding-line scheme to improve the sensitivity of this coarse grid simulation to oceanic forcing. Using spatially explicit, time varying, oceanic and atmospheric anomalies (compared to present day) from the National Center for Atmospheric Research Community Climate System Model version 3 (NCAR CCSM3; Clark et al., 2020) we run duplicate simulations for Termination 1 (T1; 20–0 ka BP) and Termination 2 (T2; 140–116 ka BP). We follow the exact same procedure as in Clark et al. (2020) and use simulations of the last glacial termination (T1) to ensure that our model can reproduce the extended glacial maximum configuration and present-day ice extent. Simulations for the penultimate glacial termination and Last Interglaciation (T2) are then run with only the climate forcing being changed. To ensure that isostatic loading of the bedrock reaches equilibrium before the start of the transient deglacial simulation we precede each of these simulations with a 20 kyr period during which a constant 'glacial maximum' climate field is applied. The conditions imposed during this phase are taken as the glacial maxima represented in the CCSM3 simulations at 140 ka and 20 ka BP for T2 and T1 respectively. Compared to Clark et al. (2020) our new simulations use an upper mantle viscosity value that is increased from $1.0\text{x}10^{19}$ Pa s to $1.3\text{x}10^{20}$ Pa s, as well as a topographic elevation correction to account for the effect of dynamic topography (Austermann et al., 2015). These modifications are implemented in an attempt to pro-

duce earlier and faster mass loss than the original simulations (Clark et al., 2020), in an attempt to reproduce the timing of AIS changes interpreted from Antarctic glaciological and geological records (Wilson et al., 2018; Turney et al., 2020). For wider context we also compare our results to inferences of AIS mass loss from other studies (Fig. 1b; Kopp et al., 2009).

Experimentation shows that the model is very sensitive to mantle viscosity and only a narrow range of values exists that allow present-day grounding lines to be matched as well as above-present LIG mass loss to be produced (Figs. S1, S2). In this paper we also present an extension of the T1 simulation in which present-day (1979–2010) basal melt rates (Bernales et al., 2017) and atmospheric forcing (Golledge et al., 2019) are maintained for an additional 4 kyr, in order to investigate the future dynamic (not climate-forced) response of the AIS.

3 Results

Figure 1 illustrates the AIS response in terms of sea-level-equivalent mass loss to deglacial environmental forcings for (a) T1 and (b) T2. Mass loss above present is first achieved shortly after 129 ka, peaking at 126 ka with a sea level contribution of 4.03 m. This ice volume minimum is maintained only briefly before a slow regrowth of the ice sheet and lowering of sea level to 118 ka, followed by renewed mass loss that continues to the end of the simulation at 116 ka. Both the timing and magnitude of peak modelled AIS mass loss are consistent with probabilistic estimates (Kopp et al., 2009) of the Southern Hemisphere sea-level contribution during this period (Fig. 1b, grey line and shading) but our modelled sea level contribution starts to exceed present-day sea level around 2000 years earlier than the Kopp et al. (2009) median. We consider this apparent mismatch acceptable, however, given that Kopp et al. (2009) caution the use of their ice volume projections on the basis that in their assessment they use a Gaussian distribution to represent a non-Gaussian prior. Other studies have inferred little or no mass loss from the WAIS prior to 128 ka BP (Holloway et al., 2016), which our simulation is also largely consistent with. The AIS contribution to GMSL in our simulation comes largely from the WAIS (Fig. 1c), primarily the Thwaites and Pine Island Glacier catchments. As a consequence of CCSM3-simulated cooler-than-present subsurface ocean temperatures in the Ross and Weddell seas (Fig. S3), both the Ross and Filchner-Ronne ice shelves remain intact. In East Antarctica our modelled grounded ice extent closely resembles

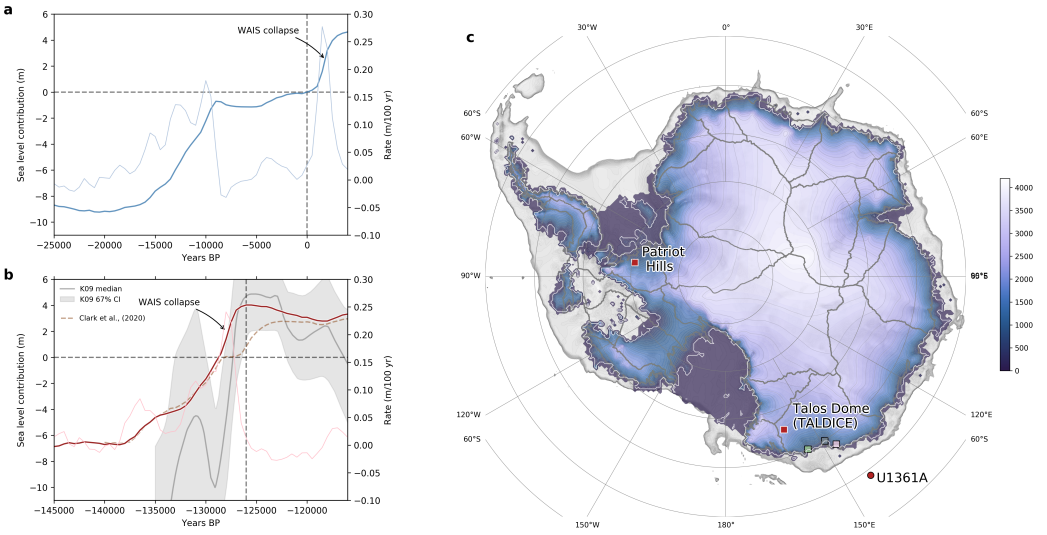

Figure 1. Simulated mass loss from the Antarctic Ice Sheet (bold lines) during a) the last and b) the penultimate glacial terminations. Rates-of-change shown with thinner lines in each panel. Modelled LIG sea-level-equivalent mass loss from Clark et al. (2020) shown with dashed brown line in b) for comparison to the new simulation. Median and 67% confidence interval of a probabilistic reconstruction of the Southern Hemisphere contribution to global mean sea level shown with grey line and shading (Kopp et al., 2009). c) Surface elevation of the modelled Antarctic Ice Sheet at 126 ka BP when peak LIG mass loss is reached. Patriot Hills blue ice area, Talos Dome ice core site, and U1361A marine sediment core location and the three sites (coloured boxes) investigated in Figure 4 also shown.

its present-day configuration, with no substantial grounding line retreat apparent in either the WSB, the Aurora Basin, or the Recovery catchment.

Closer investigation of the Amundsen Sea Embayment reveals that the retreating grounding line in this area migrates inland of its present-day position shortly after 130 ka BP and progressively evacuates the interior of WAIS over the subsequent 3–4 kyr (Fig. 2). Grounded ice in the Weddell Sea embayment appears to retreat to close to its present-day extent in the millennia just before and just after 130 ka, and then stabilises. Comparison of modelled grounding-line positions in the Weddell and Amundsen Sea sectors highlights the far more rapid retreat in the latter than the former, consistent with previous interpretations of LIG marine ice sheet instability in this sector (Clark et al., 2020). The more rapid retreat we simulate than modelled previously (Fig. 1b) arises from our

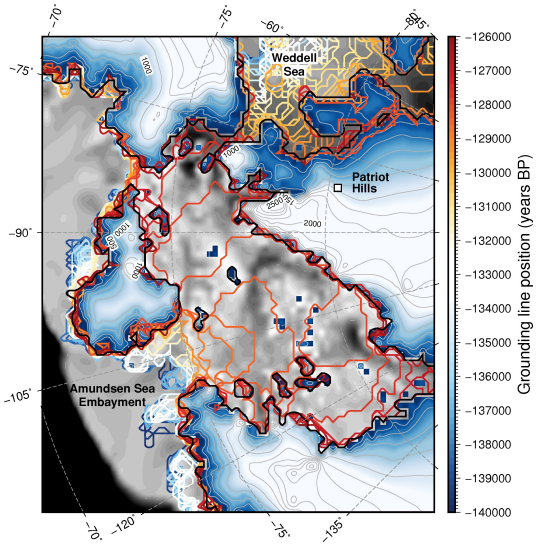

Figure 2. Grounding line retreat in the Amundsen Sea Embayment from 140–126 ka BP. Retreat proceeds rapidly into the interior of WAIS once the pinning point near the present-day grounding line is lost. Grounding line retreat in the Weddell Sea is by comparison much slower, but takes place earlier. Location of Patriot Hills ice core record (Turney et al., 2020) also shown.

stiffer mantle parameterisation ('Methods', above), leading to slower isostatic rebound that gives rise to deeper water during WAIS retreat.

To gauge the degree of fit between our simulation and two empirical studies that report isotopic evidence of changes in the AIS during the LIG, we first consider the isotope record recovered from the Blue Ice Area (BIA) of Horseshoe Valley, in the Patriot Hills of West Antarctica (278.65° E, 80.3° S, Figs. 1c & 2; Turney et al., 2020). The ice core preserves a tephra layer geochemically correlated to a tephra in the Dome Fuji ice core dated to 130.7 ± 1.8 ka BP (Hillenbrand et al., 2008). Stratigrapically above this horizon ice younger than ca. 130 ka, but older than 80 ka, is absent, implying either a hiatus in accumulation, or post-depositional loss. Our simulation predicts a 5000-year long episode of ice thinning coincident with the timing of tephra deposition and the beginning of the isotopic hiatus (Fig. 3a). If this thinning had been driven by surface ablation (wind-induced sublimation) the tephra would not be preserved in situ. Conversely, if thinning were instead primarily the result of melting at the bed rather than at the surface, the tephra should be preserved beneath younger ice, yet this is not the case.

In our simulation the onset of thinning appears to be a response to a steady increase in surface velocity that started around 132.5 ka BP (Fig. 3b, red line). This date corresponds to the timing of southward retreat of the ice sheet grounding line in the Weddell Sea (Fig. 2) that triggered regional uplift at the BIA site from ca. 131 ka BP (Fig. 3b, blue line). Combined with collapse of the ASE glaciers from 129 ka (Fig. 2) the reduction in regional ice loading led to accelerated bedrock rebound and promoted faster basal sliding due to the increase in topographic gradient (Fig. 3b, black line).

Since modelled surface velocities are an order of magnitude greater than the rate of basal sliding, flow occurred primarily by shear (internal deformation). Under this kind of flow regime, the increasing surface slope and surface velocity driven by Weddell Sea grounding line retreat and bedrock uplift would have led to preferential thinning near the surface rather than in deeper ice layers. Thinning rates increased gradually from 132.5 ka BP reaching a maximum of around 0.5 m/year by ca. 128.5 ka BP (Fig. 3a). Snow layers accumulating during this time would have thus become increasingly thinned, relative to older layers beneath, as they flowed from their original location to the BIA sample site downstream. In this scenario, the apparent hiatus actually may represent a period of enhanced layer thinning that allowed stratigraphically separated isochrones to eventually intersect (Fig. 3c). Although our simulations do not extend to 80 ka BP, we surmise that thinning halted at 80 ka because of renewed isostatic loading due to ASE regrowth, and/or because of readvance of Weddell Sea grounding lines as the climate cooled.

Many studies have considered the possibility that the WSB in East Antarctica could have collapsed during warmer periods of the past (Cook et al., 2013; Mengel & Levermann, 2014; Patterson et al., 2014; Golledge, Thomas, et al., 2017; Bertram et al., 2018). Yet direct evidence pertinent to the LIG is lacking, and the most proximal record of ice sheet change in this area is marine sediment core U1361A at 143.89°E, 64.41°S (Wilson et al., 2018). This archive preserves IBRD that includes detrital sediments whose radiogenic values reflect different source areas. A third sedimentary proxy, the barium/aluminium ratio of laminated clays, indicates changes in sea ice extent and biological productivity. Co-variance of these markers has been used to suggest that reduced sea ice during Pleistocene interglacials was coincident with increased sediment erosion from the WSB, perhaps because of retreat of the ice margin (Wilson et al., 2018). Inland terrestrial geochemical records, however, suggest that the WSB has been ice-filled since c. 400 ka BP

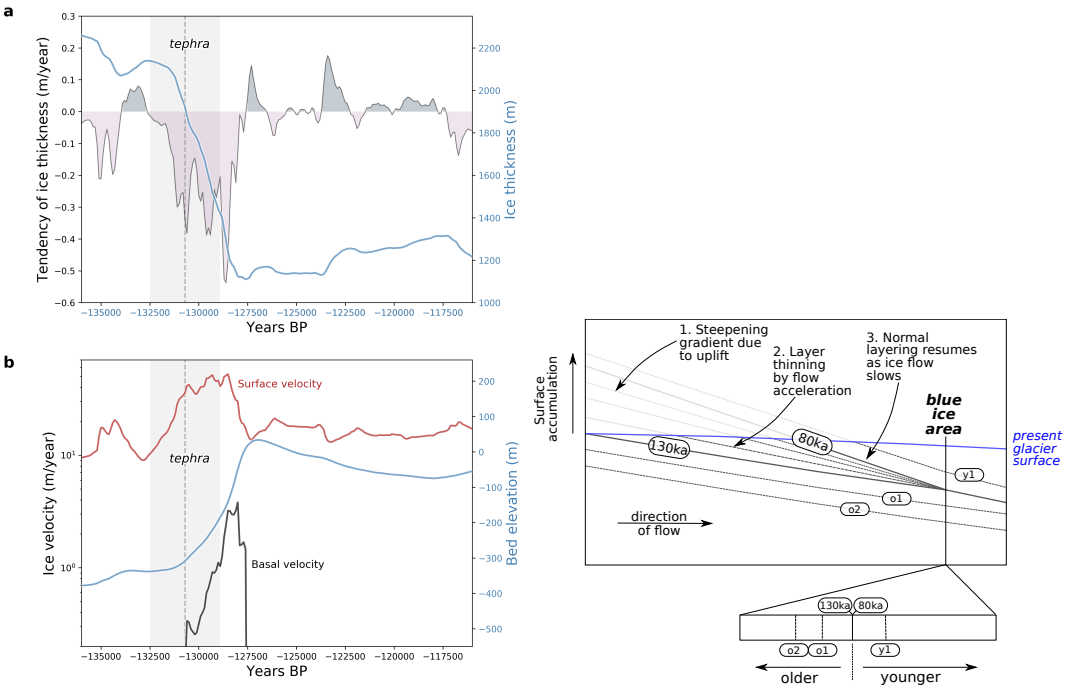

Figure 3. a) Modelled ice thickness and its rate of change, and b) bed elevation, and surface and basal velocity at the Patriot Hills blue ice area through the period 132–116 ka BP. Timing of tephra horizon marking the beginning of the hiatus in the core (Turney et al., 2020) also shown (dotted line), including age uncertainty (grey shading). c) Schematic explanation of the mechanism leading to the c. 130–80 ka BP hiatus in the Patriot Hills ice core record. Steepening of the ice surface due to bedrock uplift and grounding-line retreat lead to enhancing thinning as ice is advected more quickly downglacier, eventually allowing time-separated ice layers (isochrones) to converge.

(Blackburn et al., 2020), and hence if it did contribute to higher-than-present LIG GMSL, the contribution may have been relatively minor. Recent high-resolution ice sheet modelling supports this latter interpretation, showing that the isotopic record preserved in the Talos Dome ice core is inconsistent with the surface lowering of that area that would have occurred had the WSB deglaciated substantially (Sutter et al., 2020). Sutter et al. (2020) conclude that during the LIG the WSB could have contributed only up to ca. 0.8 m SLE.

Here we unify these studies. Figure 4a shows our modelled ice surface elevation over the WSB during the LIG, at 126 ka BP when modelled Antarctic ice loss peaked. Modelled surface elevation change at Talos Dome from 132 – 116 ka is shown (blue line) in Figure 4c, and indicates changes of approximately 100 m over 10000 years, consistent with the TALDICE reconstruction (Sutter et al., 2020). We also track changes in ice elevation and basal ice velocity in the key outlet glaciers of this region: Cook, Ninnis, and Mertz (Fig. 4e,f). Even in the absence of grounding-line retreat in this area we simulate thinning of up to 500 m in the trunk of the Ninnis Glacier, coupled with an abrupt increase in sliding velocity from approximately 150 m/year to 450 m/year. Because these accelerations are localised, however, the sea-level equivalent volume of this catchment is only 0.05 m less than in our modelled present-day geometry. Our modelled ice dynamic changes are coeval with the proxy-based interpretations of ice sheet changes (Fig. 4d,e,f). Since basal erosion and subglacial sediment transport are largely controlled by sliding velocity (Pollard & DeConto, 2003; Herman et al., 2015), our modelled changes can plausibly explain the increase in basal erosion inferred from an inland subglacial source and transported to the offshore marine sediment core U1361A (Wilson et al., 2018).

4 Implications for future change

A striking feature of our T1 tuning experiment (Fig. 1a) is that after a period of relative stability during the Holocene (approximately the last 10,000 years), our model predicts renewed, and rapid, AIS mass loss beginning c. 1500 years after present day. The trajectory of ice loss over the period 1500-4000 years into the future is similar to the pattern of loss taking place during the early millennia of the LIG (Fig. 1b), reflecting MISI-forced collapse of the ASE sector of WAIS. Given that no additional environmental forcing is applied during this period (from year 0 into the future), the lagged response is most likely a consequence of our basal melt parameterisation, which is opti-

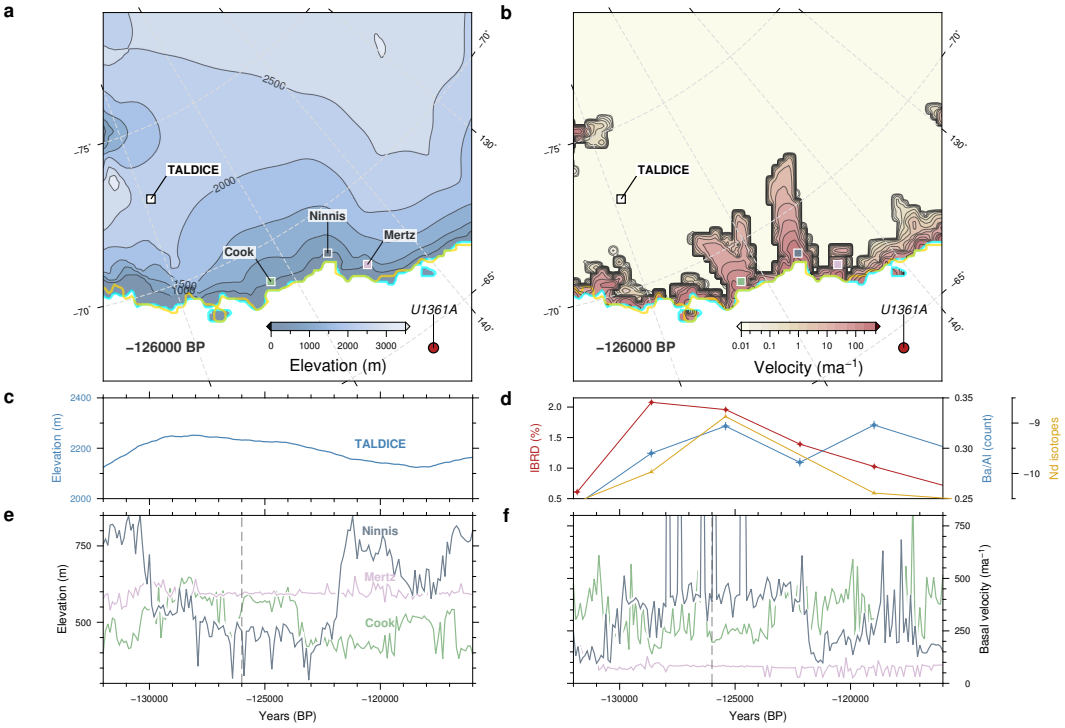

Figure 4. Ice thickness and basal ice velocity changes in the Wilkes Subglacial Basin during the period 132–116ka BP. a) Modelled ice elevation and b) basal ice velocity at 126 ka BP showing location of the three main outlet glaciers in this region. Location of the Talos Dome ice core site (TALDICE) and marine sediment core U1361A also shown. Gold and cyan lines shows present-day and 126 ka BP grounding-line positions respectively. c) Timeseries of modelled ice elevation changes and d) sediment proxies from U1361A compared to e) modelled elevation and f) basal velocity changes at the three glacier trunks shown in a). The model predicts substantial thinning and acceleration of Ninnis Glacier coincident with increased sediment flux to U1361A, yet without impact on ice thickness at Talos Dome. Vertical dotted lines identify the timeslice shown in panels a) and b)

mised to closely reproduce present-day (1979–2010) melt rates (Bernales et al., 2017; Golledge et al., 2019). The implication therefore is that ocean warming to-date is already sufficient to trigger millennial-scale collapse of part of West Antarctica, as has been found previously (Joughin et al., 2014; Arthern & Williams, 2017; Golledge et al., 2019).

5 Conclusions

We have presented new transient simulations of the AIS through both the most recent, and the penultimate, deglaciations, the current interglaciation and the LIG. Our model is parameterised to reproduce the most recent glacial maximum expansion as well as present-day AIS configuration, and then by only changing the climatological forcing also predicts changes in LIG ice sheet geometry and dynamics that can explain three independent ice-proximal proxy records as well as probabilistic estimates of LIG changes in GMSL. The same simulations also suggest that the present-day AIS is already primed for MISI-driven retreat over coming millennia, or sooner if additional environmental forcing is imposed.

Acknowledgments

Ice sheet model outputs shown in this paper are available at the Open Science Framework (https://osf.io.xxx). NRG acknowledges funding from Royal Society of New Zealand contract VUW-1501. Simulations on which this work is based were funded by US National Science Foundation (NSF) through grant numbers AGS-1503032 (to PUC and AEC), AGS-1502990 (to FH), 1559040 (to AD) and OPP-1443437 (to AEC). FH gratefully acknowledges the NOAA Climate and Global Change Postdoctoral Fellowship programme, administered by the University Corporation for Atmospheric Research. High-performance computing support from Yellowstone (ark:/85065/d7wd3xhc) and Cheyenne (doi:10.5065/D6RX99HX) was provided by NCARs Computational and Information Systems Laboratory, sponsored by the NSF. This research used resources of the Oak Ridge Leadership Computing Facility at the Oak Ridge National Laboratory, which is supported by the Office of Science of the US Department of Energy under contract number DE-AC05-00OR22725. CSMT and CJF acknowledge support from the Australian Research Council (ARC), including Linkage Project (LP120200724), supported by Linkage Partner Antarctic Logistics and Expeditions. NRG, TRN, RHL, RMM, DPL, NANB and GBD acknowledge support from Ministry for Business, Innovation and Employment contracts RTUV1705 ('NZSeaRise')

and ANTA1801 ('Antarctic Science Platform'). PISM is supported by NASA grant numbers NNX13AM16G and NNX13AK27G. The authors declare no financial conflicts of interest.

References

Albrecht, T., Winkelmann, R., & Levermann, A. (2020). Glacial-cycle simulations of the Antarctic Ice Sheet with the Parallel Ice Sheet Model (PISM)–Part 1: Boundary conditions and climatic forcing. *The Cryosphere*, *14*(2).

Arthern, R. J., & Williams, C. R. (2017). The sensitivity of West Antarctica to the submarine melting feedback. *Geophysical Research Letters*, *44*(5), 2352–2359.

Aschwanden, A., Fahnestock, M. A., Truffer, M., Brinkerhoff, D. J., Hock, R., Khroulev, C., ... Khan, S. A. (2019). Contribution of the Greenland Ice Sheet to sea level over the next millennium. *Science Advances*, *5*(6), eaav9396.

Austermann, J., Pollard, D., Mitrovica, J. X., Moucha, R., Forte, A. M., DeConto, R. M., ... Raymo, M. E. (2015). The impact of dynamic topography change on Antarctic ice sheet stability during the mid-Pliocene warm period. *Geology*, *43*(10), 927–930.

Bernales, J., Rogozhina, I., & Thomas, M. (2017). Melting and freezing under Antarctic ice shelves from a combination of ice-sheet modelling and observations. *Journal of Glaciology*, *63*, 731-744.

Bertram, R. A., Wilson, D. J., van de Flierdt, T., McKay, R. M., Patterson, M. O., Jimenez-Espejo, F. J., ... Riesselman, C. R. (2018). Pliocene deglacial event timelines and the biogeochemical response offshore Wilkes Subglacial Basin, East Antarctica. *Earth and Planetary Science Letters*, *494*, 109–116.

Blackburn, T., Edwards, G. H., Tulaczyk, S., Scudder, M., Piccione, G., Hallet, B., ... Babbe, J. T. (2020). Ice retreat in Wilkes Basin of East Antarctica during a warm interglacial. *Nature*, *583*, 554-559.

Bradley, S. L., Reerink, T. J., Van De Wal, R. S., & Helsen, M. M. (2018). Simulation of the Greenland Ice Sheet over two glacial-interglacial cycles: investigating a sub-ice-shelf melt parameterization and relative sea level forcing in an ice-sheet-ice-shelf model. *Climate of the Past*, *14*(5), 619–635.

Brook, E. J., White, J. W., Schilla, A. S., Bender, M. L., Barnett, B., Severinghaus, J. P., ... Steig, E. J. (2005). Timing of millennial-scale climate change at Siple

Dome, West Antarctica, during the last glacial period. *Quaternary Science Reviews*, *24*(12-13), 1333–1343.

Bueler, E., & Brown, J. (2009). Shallow shelf approximation as a "sliding law" in a thermomechanically coupled ice sheet model. *Journal of Geophysical Research*, *114*, F03008.

Buizert, C., Adrian, B., Ahn, J., Albert, M., Alley, R. B., Baggenstos, D., ... others (2015). Precise interpolar phasing of abrupt climate change during the last ice age. *Nature*, *520*(7549), 661–665.

Calov, R., Robinson, A., Perrette, M., & Ganopolski, A. (2015). Simulating the Greenland ice sheet under present-day and palaeo constraints including a new discharge parameterization. *The Cryosphere*, *9*, 179–196.

Capron, E., Govin, A., Feng, R., Otto-Bliesner, B. L., & Wolff, E. (2017). Critical evaluation of climate syntheses to benchmark cmip6/pmip4 127 ka last interglacial simulations in the high-latitude regions. *Quaternary Science Reviews*, *168*, 137–150.

Chadwick, M., Allen, C., Sime, L., & Hillenbrand, C.-D. (2020). Analysing the timing of peak warming and minimum winter sea-ice extent in the Southern Ocean during MIS 5e. *Quaternary Science Reviews*, *229*, 106134.

Clark, P. U., He, F., Golledge, N. R., Mitrovica, J. X., Dutton, A., Hoffman, J. S., & Dendy, S. (2020). Oceanic forcing of penultimate deglacial and last interglacial sea-level rise. *Nature*, *577*, 660-664.

Colville, E. J., Carlson, A. E., Beard, B. L., Hatfield, R. G., Stoner, J. S., Reyes, A. V., & Ullman, D. J. (2011). Sr-Nd-Pb Isotope Evidence for Ice-Sheet Presence on Southern Greenland During the Last Interglacial. *Science*, *333*, 620-623.

Cook, C. P., van de Flierdt, T., Williams, T., Hemming, S. R., Iwai, M., Kobayashi, M., ... others (2013). Dynamic behaviour of the East Antarctic ice sheet during Pliocene warmth. *Nature Geoscience*, *6*(9), 765–769.

Dahl-Jensen, D., Albert, M., Aldahan, A., Azuma, N., Balslev-Clausen, D., Baumgartner, M., ... others (2013). Eemian interglacial reconstructed from a Greenland folded ice core. *Nature*, *493*(7433), 489.

DeConto, R., & Pollard, D. (2016). Contribution of Antarctica to past and future sea-level rise. *Nature*, *531*, 591-597.

Dutton, A., Carlson, A., Long, A., Milne, G., Clark, P., DeConto, R., ... Raymo, M. (2015). Sea-level rise due to polar ice-sheet mass loss during past warm periods. *Science*, *349*, aaa4019.

Feldmann, J., & Levermann, A. (2015). Interaction of marine ice-sheet instabilities in two drainage basins: simple scaling of geometry and transition time. *The Cryosphere*, *9*, 631–645.

Fischer, H., Meissner, K. J., Mix, A. C., Abram, N. J., Austermann, J., Brovkin, V., ... others (2018). Palaeoclimate constraints on the impact of 2°c anthropogenic warming and beyond. *Nature Geoscience*, *11*(7), 474.

Fudge, T., Steig, E. J., Markle, B. R., Schoenemann, S. W., Ding, Q., Taylor, K. C., ... others (2013). Onset of deglacial warming in West Antarctica driven by local orbital forcing. *Nature*, *500*(7463), 440–444.

Goelzer, H., Huybrechts, P., Loutre, M.-F., & Fichefet, T. (2016). Last Interglacial climate and sea-level evolution from a coupled ice sheet–climate model. *Climate of the Past*, *12*(12), 2195–2213.

Golledge, N. R., Keller, E. D., Gomez, N., Naughten, K. A., Bernales, J., Trusel, L. D., & Edwards, T. L. (2019). Global environmental consequences of twenty-first-century ice-sheet melt. *Nature*, *566*, 65-72.

Golledge, N. R., Levy, R. H., McKay, R. M., & Naish, T. R. (2017). East Antarctic ice sheet most vulnerable to Weddell Sea warming. *Geophysical Research Letters*, *44*, 2343–2351.

Golledge, N. R., Menviel, L., Carter, L., Fogwill, C., England, M., Cortese, G., & Levy, R. (2014). Antarctic contribution to meltwater pulse 1A from reduced Southern Ocean overturning. *Nature Communications*, *(5)*, 1-10. doi: doi:10.1038/ncomms6107

Golledge, N. R., Thomas, Z., Levy, R., Gasson, E., Naish, T., McKay, R., ... Fogwill, C. (2017). Antarctic climate and ice sheet configuration during a peak-warmth Early Pliocene interglacial. *Climate of the Past*, *13*, 959975.

Herman, F., Beyssac, O., Brughelli, M., Lane, S. N., Leprince, S., Adatte, T., ... Cox, S. C. (2015). Erosion by an Alpine glacier. *Science*, *350*(6257), 193–195.

Hillenbrand, C.-D., Moreton, S., Caburlotto, A., Pudsey, C., Lucchi, R., Smellie, J., ... Larter, R. (2008). Volcanic time-markers for Marine Isotopic Stages 6 and 5 in Southern Ocean sediments and Antarctic ice cores: implications for tephra

correlations between palaeoclimatic records. *Quaternary Science Reviews*, *27*(5-6), 518–540.

Hoffman, J. S., Clark, P. U., Parnell, A. C., & He, F. (2017). Regional and global sea-surface temperatures during the last interglaciation. *Science*, *355*(6322), 276–279.

Holloway, M. D., Sime, L. C., Singarayer, J. S., Tindall, J. C., Bunch, P., & Valdes, P. J. (2016). Antarctic last interglacial isotope peak in response to sea ice retreat not ice-sheet collapse. *Nature Communications*, *7*(1), 1–9.

Joughin, I., Smith, B. E., & Medley, B. (2014). Marine Ice Sheet Collapse Potentially Under Way for the Thwaites Glacier Basin, West Antarctica. *Science*, *344*, 735-738.

Kopp, R. E., Simons, F. J., Mitrovica, J. X., Maloof, A. C., & Oppenheimer, M. (2009, December). Probabilistic assessment of sea level during the last interglacial stage. *Nature*, *462*(7275), 863–867. doi: 10.1038/nature08686

Korotkikh, E. V., Mayewski, P. A., Handley, M. J., Sneed, S. B., Introne, D. S., Kurbatov, A. V., ... McIntosh, W. C. (2011). The last interglacial as represented in the glaciochemical record from Mount Moulton Blue Ice Area, West Antarctica. *Quaternary Science Reviews*, *30*(15-16), 1940–1947.

Landais, A., Masson-Delmotte, V., Capron, E., Langebroek, P. M., Bakker, P., Stone, E. J., ... others (2016). How warm was Greenland during the last interglacial period? *Climate of the Past*, *12*(9), 1933–1948.

Marino, G., Rohling, E., Rodriguez-Sanz, L., Grant, K., Heslop, D., Roberts, A., ... Yu, J. (2015). Bipolar seesaw control on last interglacial sea level. *Nature*, *522*, 197-201.

Marzeion, B., Hock, R., Anderson, B., Bliss, A., Champollion, N., Fujita, K., ... others (2020). Partitioning the uncertainty of ensemble projections of global glacier mass change. *Earth's Future*, e2019EF001470.

Masson-Delmotte, V., Schulz, M., Abe-Ouchi, A., Beer, J., Ganopolski, A., González Rouco, J., ... Timmermann, A. (2013). Information from Paleoclimate Archives. In T. Stocker et al. (Eds.), *Climate Change 2013 : The Physical Science Basis. Contribution of Working Group I to the Fifth Assessment Report of the Intergovernmental Panel on Climate Change* (p. 383-464).

Mengel, M., & Levermann, A. (2014). Ice plug prevents irreversible discharge from

East Antarctica. *Nature Climate Change*, *4*, 451–455.

Mulvaney, R., Triest, J., & Alemany, O. (2014). The James Ross Island and the Fletcher Promontory ice-core drilling projects. *Annals of Glaciology*, *55*(68), 179–188.

Patterson, M., McKay, R., Naish, T., Escutia, C., Jimenez-Espejo, F., Raymo, M., ... IODP Expedition 318 scientists (2014). Orbital forcing of the East Antarctic ice sheet during the Pliocene and Early Pleistocene. *Nature Geoscience*, *7*, 841–847.

Pollard, D., & DeConto, R. M. (2003). Antarctic ice and sediment flux in the Oligocene simulated by a climate-ice sheet-sediment model. *Palaeogeography, Palaeoclimatology, Palaeoecology*, *198*, 53–67.

Rohling, E. J., Hibbert, F. D., Grant, K. M., Galaasen, E. V., Irvalı, N., Kleiven, H. F., ... others (2019). Asynchronous Antarctic and Greenland ice-volume contributions to the last interglacial sea-level highstand. *Nature Communications*, *10*(1), 1–9.

Seguinot, J., Khroulev, C., Rogozhina, I., Stroeven, A. P., & Zhang, Q. (2014). The effect of climate forcing on numerical simulations of the Cordilleran ice sheet at the Last Glacial Maximum. *The Cryosphere*, *8*, 1087–1103.

Shackleton, S., Baggenstos, D., Menking, J., Dyonisius, M., Bereiter, B., Bauska, T., ... others (2020). Global ocean heat content in the Last Interglacial. *Nature Geoscience*, *13*(1), 77–81.

Sutter, J., Eisen, O., Werner, M., Grosfeld, K., Kleiner, T., & Fischer, H. (2020). Limited retreat of the Wilkes Basin ice sheet during the Last Interglacial. *Geophysical Research Letters*, *47*(13), e2020GL088131.

Sutter, J., Gierz, P., Grosfeld, K., Thoma, M., & Lohmann, G. (2016). Ocean temperature thresholds for last interglacial West Antarctic ice sheet collapse. *Geophysical Research Letters*, *43*(6), 2675–2682.

Turney, C., Fogwill, C., Golledge, N., McKay, N. P., van Sebille, E., Jones, R. T., ... others (2020). Early Last Interglacial ocean warming drove substantial ice mass loss from Antarctica. *Proceedings of the National Academy of Sciences*, *117*(8), 3996–4006.

Turney, C., & Jones, R. (2010). Does the Agulhas Current amplify global temperatures during super-interglacials? *Journal of Quaternary Science*, *25*, 839-843.

Wilson, D. J., Bertram, R. A., Needham, E. F., van de Flierdt, T., Welsh, K. J., McKay, R. M., ... Escutia, C. (2018). Ice loss from the East Antarctic Ice Sheet during late Pleistocene interglacials. *Nature*, *561*(7723), 383–386.

Winkelmann, R., Levermann, A., Ridgwell, A., & Caldeira, K. (2015). Combustion of available fossil fuel resources sufficient to eliminate the Antarctic Ice Sheet. *Science Advances*, *1*, e1500589.

Winkelmann, R., Martin, M. A., Haseloff, M., Albrecht, T., Bueler, E., Khroulev, C., & Levermann, A. (2010, August). The Potsdam Parallel Ice Sheet Model (PISM-PIK) - Part 1: Model description. *The Cryosphere*, *5*, 715–726.

Yau, A. M., Bender, M. L., Robinson, A., & Brook, E. J. (2016). Reconstructing the last interglacial at Summit, Greenland: Insights from GISP2. *Proceedings of the National Academy of Sciences*, *113*(35), 9710–9715.